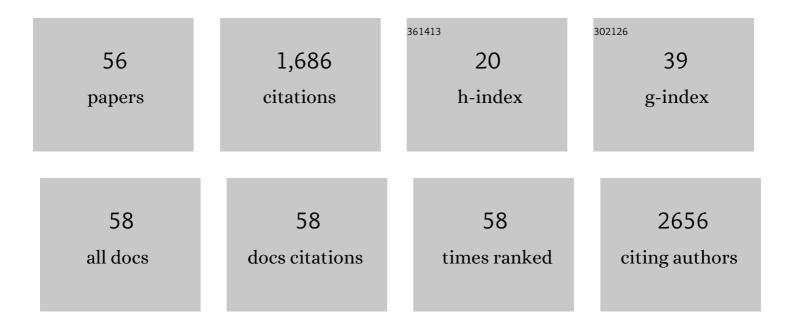
Jikai Wen

List of Publications by Year in descending order

Source: https://exaly.com/author-pdf/4315886/publications.pdf Version: 2024-02-01



#	Article	IF	CITATIONS
1	Inhibition of EZH2 and activation of ERRÎ ³ synergistically suppresses gastric cancer by inhibiting FOXM1 signaling pathway. Gastric Cancer, 2021, 24, 72-84.	5.3	16
2	Antimicrobial resistance, virulence characteristics and genotypes of Bacillus spp. from probiotic products of diverse origins. Food Research International, 2021, 139, 109949.	6.2	24
3	Influenza A virus protein PAâ€X suppresses host Ankrd17â€mediated immune responses. Microbiology and Immunology, 2021, 65, 48-59.	1.4	3
4	Cell fate determined by the activation balance between PKR and SPHK1. Cell Death and Differentiation, 2021, 28, 401-418.	11.2	10
5	Quantitative proteomics implicates YggT in streptomycin resistance in Salmonella enterica serovar Enteritidis. Biotechnology Letters, 2021, 43, 919-932.	2.2	4
6	New Insights into the Virulence Traits and Antibiotic Resistance of Enterococci Isolated from Diverse Probiotic Products. Microorganisms, 2021, 9, 726.	3.6	6
7	Role of DNA methylationâ€related chromatin remodeling in aryl hydrocarbon receptorâ€dependent regulation of Tâ€2 toxin highly inducible <i>Cytochrome P450 1A4</i> gene. FASEB Journal, 2021, 35, e21469.	0.5	4
8	Indoor bacterial, fungal and viral species and functional genes in urban and rural schools in Shanxi Province, China–association with asthma, rhinitis and rhinoconjunctivitis in high school students. Microbiome, 2021, 9, 138.	11.1	34
9	Cereulide Exposure Caused Cytopathogenic Damages of Liver and Kidney in Mice. International Journal of Molecular Sciences, 2021, 22, 9148.	4.1	3
10	Chronic cereulide exposure causes intestinal inflammation and gut microbiota dysbiosis in mice. Environmental Pollution, 2021, 288, 117814.	7.5	11
11	Baiting out a full length sequence from unmapped RNA-seq data. BMC Genomics, 2021, 22, 857.	2.8	3
12	Transcriptome analysis of golden pompano (Trachinotus ovatus) liver indicates a potential regulatory target involved in HUFA uptake and deposition. Comparative Biochemistry and Physiology Part D: Genomics and Proteomics, 2020, 33, 100633.	1.0	10
13	Supreme Catalytic Properties of Enzyme Nanoparticles Based on Ferritin Self-Assembly. ACS Applied Bio Materials, 2020, 3, 7158-7167.	4.6	5
14	Deoxynivalenol Exposure Suppresses Adipogenesis by Inhibiting the Expression of Peroxisome Proliferator-Activated Receptor Gamma 2 (PPARγ2) in 3T3-L1 Cells. International Journal of Molecular Sciences, 2020, 21, 6300.	4.1	4
15	Cloning, molecular characterization, and nutritional regulation of fatty acid-binding protein family genes in gold pompanos (Trachinotus ovatus). Comparative Biochemistry and Physiology - B Biochemistry and Molecular Biology, 2020, 246-247, 110463.	1.6	11
16	Dual Function of a Novel Bacterium, Slackia sp. D-G6: Detoxifying Deoxynivalenol and Producing the Natural Estrogen Analogue, Equol. Toxins, 2020, 12, 85.	3.4	25
17	Lactobacillus rhamnosus GG supplementation modulates the gut microbiota to promote butyrate production, protecting against deoxynivalenol exposure in nude mice. Biochemical Pharmacology, 2020, 175, 113868.	4.4	61
18	Identification of NOVA family proteins as novel β-catenin RNA-binding proteins that promote epithelial-mesenchymal transition. RNA Biology, 2020, 17, 881-891.	3.1	16

Jikai Wen

#	Article	IF	CITATIONS
19	Deoxynivalenol globally affects the selection of 3' splice sites in human cells by suppressing the splicing factors, U2AF1 and SF1. RNA Biology, 2020, 17, 584-595.	3.1	2
20	Aromatic hydrocarbon receptor regulates chicken cytochrome P450 1A5 transcription: A novel insight into T-2 toxin-induced gene expression and cytotoxicity in LMH cells. Biochemical Pharmacology, 2019, 168, 319-329.	4.4	15
21	T-2 toxin upregulates the expression of human cytochrome P450 1A1 (CYP1A1) by enhancing NRF1 and Sp1 interaction. Toxicology Letters, 2019, 315, 77-86.	0.8	10
22	Variable protein homeostasis in housekeeping and non-housekeeping pathways under mycotoxins stress. Scientific Reports, 2019, 9, 7819.	3.3	7
23	T-2 toxin inhibits the production of mucin via activating the IRE1/XBP1 pathway. Toxicology, 2019, 424, 152230.	4.2	35
24	AhR regulates the expression of human cytochrome P450 1A1 (<i>CYP1A1</i>) by recruiting Sp1. FEBS Journal, 2019, 286, 4215-4231.	4.7	37
25	Deoxynivalenol induces inhibition of cell proliferation via the Wnt/β-catenin signaling pathway. Biochemical Pharmacology, 2019, 166, 12-22.	4.4	26
26	Multiple CH/İ∈ Interactions Maintain the Binding of Aflatoxin B1 in the Active Cavity of Human Cytochrome P450 1A2. Toxins, 2019, 11, 158.	3.4	9
27	Coordinated Transcriptional Regulation of Cytochrome P450 3As by Nuclear Transcription Factor Y and Specificity Protein 1. Molecular Pharmacology, 2019, 95, 507-518.	2.3	5
28	Detoxification of trichothecene mycotoxins by a novel bacterium, Eggerthella sp. DII-9. Food and Chemical Toxicology, 2018, 112, 310-319.	3.6	59
29	C9orf140, a novel Axin1-interacting protein, mediates the negative feedback loop of Wnt/β-catenin signaling. Oncogene, 2018, 37, 2992-3005.	5.9	15
30	Sp1, Instead of AhR, Regulates the Basal Transcription of Porcine CYP1A1 at the Proximal Promoter. Frontiers in Pharmacology, 2018, 9, 927.	3.5	4
31	The critical role of porcine cytochrome P450 3A46 in the bioactivation of aflatoxin B1. Biochemical Pharmacology, 2018, 156, 177-185.	4.4	12
32	JNK-AKT-NF-κB controls P-glycoprotein expression to attenuate the cytotoxicity of deoxynivalenol in mammalian cells. Biochemical Pharmacology, 2018, 156, 120-134.	4.4	25
33	Carrier-Mediated and Energy-Dependent Uptake and Efflux of Deoxynivalenol in Mammalian Cells. Scientific Reports, 2017, 7, 5889.	3.3	20
34	Bioactivation and Regioselectivity of Pig Cytochrome P450 3A29 towards Aflatoxin B1. Toxins, 2016, 8, 267.	3.4	19
35	T-2 toxin induces the expression of porcine CYP3A22 via the upregulation of the transcription factor, NF-Y. Biochimica Et Biophysica Acta - General Subjects, 2016, 1860, 2191-2201.	2.4	11
36	Mycotoxins: cytotoxicity and biotransformation in animal cells. Toxicology Research, 2016, 5, 377-387.	2.1	60

Jikai Wen

#	Article	IF	CITATIONS
37	Role of Specificity Protein 1, Hepatocyte Nuclear Factor 1 <i>α</i> , and Pregnane X Receptor in the Basal and Rifampicin-Induced Transcriptional Regulation of Porcine Cytochrome P450 3A46. Drug Metabolism and Disposition, 2015, 43, 1458-1467.	3.3	13
38	mRNA stability in the nucleus. Journal of Zhejiang University: Science B, 2014, 15, 444-454.	2.8	21
39	Visualization of the joining of ribosomal subunits reveals the presence of 80S ribosomes in the nucleus. Rna, 2013, 19, 1669-1683.	3.5	38
40	Fluorescent protein tagging confirms the presence of ribosomal proteins at <i>Drosophila</i> polytene chromosomes. PeerJ, 2013, 1, e15.	2.0	29
41	A Sir2-Like Protein Participates in Mycobacterial NHEJ. PLoS ONE, 2011, 6, e20045.	2.5	18
42	Splicing-dependent NMD does not require the EJC in Schizosaccharomyces pombe. EMBO Journal, 2010, 29, 1537-1551.	7.8	54
43	Imaging Viral Behavior in Mammalian Cells with Selfâ€Assembled Capsid–Quantumâ€Dot Hybrid Particles. Small, 2009, 5, 718-726.	10.0	120
44	Nonsense-mediated mRNA decay (NMD) mechanisms. Nature Structural and Molecular Biology, 2009, 16, 107-113.	8.2	455
45	Altering the ribosomal subunit ratio in yeast maximizes recombinant protein yield. Microbial Cell Factories, 2009, 8, 10.	4.0	57
46	Live cell imaging of protein interactions in poliovirus RNA replication complex using fluorescence resonance energy transfer (FRET). Biochemical and Biophysical Research Communications, 2008, 368, 489-494.	2.1	5
47	Nonsense-mediated mRNA decay. Biochemical Society Transactions, 2008, 36, 514-516.	3.4	46
48	UPF1 P-body localization. Biochemical Society Transactions, 2008, 36, 698-700.	3.4	13
49	Construction and Characterization of an Anti-Prion scFv Fusion Protein Pair for Detection of Prion Protein on Antibody Chip. Analytical Letters, 2007, 40, 855-873.	1.8	1
50	Cell-Free Bioassay for Measurement of Dioxins Based on Fluorescence Enhancement of Fluorescein Isothiocyanate-Labeled DNA Probe. Analytical Chemistry, 2006, 78, 7138-7144.	6.5	16
51	Phage display mediated immuno-PCR. Nucleic Acids Research, 2006, 34, e62-e62.	14.5	71
52	Construction and characterization of different MutS fusion proteins as recognition elements of DNA chip for detection of DNA mutations. Biosensors and Bioelectronics, 2005, 21, 135-144.	10.1	6
53	Visualizing the dynamic behavior of poliovirus plus-strand RNA in living host cells. Nucleic Acids Research, 2005, 33, 3245-3252.	14.5	51
54	Identification and characterization of Bacillus anthracis by multiplex PCR on DNA chip. Biosensors and Bioelectronics, 2004, 20, 807-813.	10.1	25

IKAI	N L	
	-1/1	/ H N
 INAL	~ ~ ~	

A visual DNA chip for simultaneous detection of hepatitis B virus, hepatitis C virus and human immunodeficiency virus type-1. Biosensors and Bioelectronics, 2004, 19, 685-692.	#	Article	IF	CITATIONS
	55	A visual DNA chip for simultaneous detection of hepatitis B virus, hepatitis C virus and human immunodeficiency virus type-1. Biosensors and Bioelectronics, 2004, 19, 685-692.	10.1	20

56 Distinct gut microbiota and health outcomes in asymptomatic infection, viral nucleic acid test reâ
épositive, and convalescent COVIDâ
é19 cases. , 0, , .